Supplementary Information

A Universal Supramolecular Assembly Strategy for Achieving Efficient Tunable White Emission and Anti-counterfeiting in Antimony doped Tin(IV)-based Vacancy-Ordered Double Perovskites

Minghui Lu,[a] Hui Peng,*[a] Qilin Wei,[b] Shichao Zhou,[a] Yongrun Dong,[a] Shuiyue Yu,[a] Jialong Zhao,[c] Xianci Zhong[d] and Bingsuo Zou*[a]

[a]*State Key Laboratory of Featured Metal Materials and Life-cycle Safety for Composite Structures, MOE Key Laboratory of New Processing Technology for Nonferrous Metals and Materials, and School of Resources, Environment and Materials, Guangxi University, Nanning 530004, China.*

[b]*School of Chemistry and Chemical Engineering, Shandong University, Jinan 250100, China.*

[c]*School of Physical Science and Technology, Guangxi University, Nanning 530004, China.*

[d]*Key Laboratory of Disaster Prevention and Structural Safety of Ministry of Education, Guangxi University, Nanning 530004, China*

*Email: penghuimaterial@163.com (Hui Peng); zoubs@gxu.edu.cn (Bingsuo Zou)

Table S1. Elemental analysis of Sb/(Sn+Sb) ratio in $(CsC)_2SnCl_6:Sb^{3+}$ single crystal via EDS.

Feed ratio	Sn	Sb	Measured ratio
1 %	6.66	0.28	4.035 %
5 %	8.36	0.58	6.488 %
10 %	5.76	0.49	7.767 %
20 %	5.64	1.38	19.658 %
40 %	5.34	1.81	25.315 %
60 %	6.67	1.98	22.890 %

Table S2. Elemental analysis of Sb/(Sn+Sb) ratio in $(CsC)_2SnCl_6:Sb^{3+}$ via ICP-OES.

Feed ratio	Sn	Sb	Measured ratio
1 %	111.578	6.754	5.708 %
5 %	110.033	8.531	7.195 %
10 %	105.376	11.876	10.129 %
20 %	100.200	16.026	13.789 %
40 %	88.420	21.948	19.886 %
60 %	78.237	23.997	23.468 %

Table S3. Summary of the emission wavelengths and the PL intensity ratio of **Band A** and **Band B** in Sb^{3+}-doped $(AC)_2SnCl_6$ (A = K, Rb, Cs) compounds under excitation by a Xenon lamp at 322 nm and 370 nm.

Compounds	λ_{ex} = 322 nm			λ_{ex} = 370 nm	λ_{em} = **Band A** (nm)	λ_{em} = **Band B** (nm)	Stokes Shift (nm)
	Band A (nm)	**Band B** (nm)	$I_{\textbf{Band A}}$ / $I_{\textbf{Band B}}$				
$(KC)_2SnCl_6$: Sb^{3+}	492	654	80%	654	321	370	284
$(RbC)_2SnCl_6$: Sb^{3+}	496	659	73%	657	321	370	287
$(CsC)_2SnCl_6$: Sb^{3+}	509	669	47%	662	322	368	294

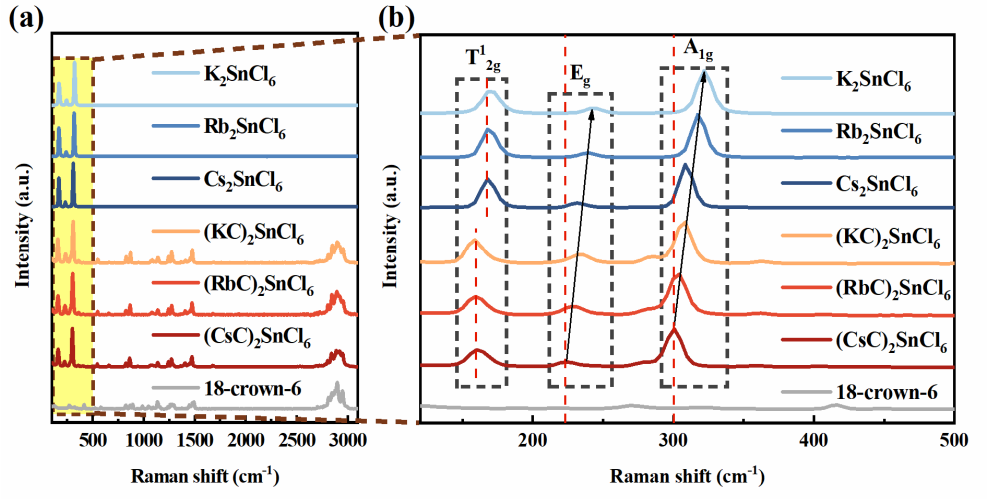

Fig. S1 Raman spectra of 18-crown-6 ether, A_2SnCl_6 and $(AC)_2SnCl_6$.

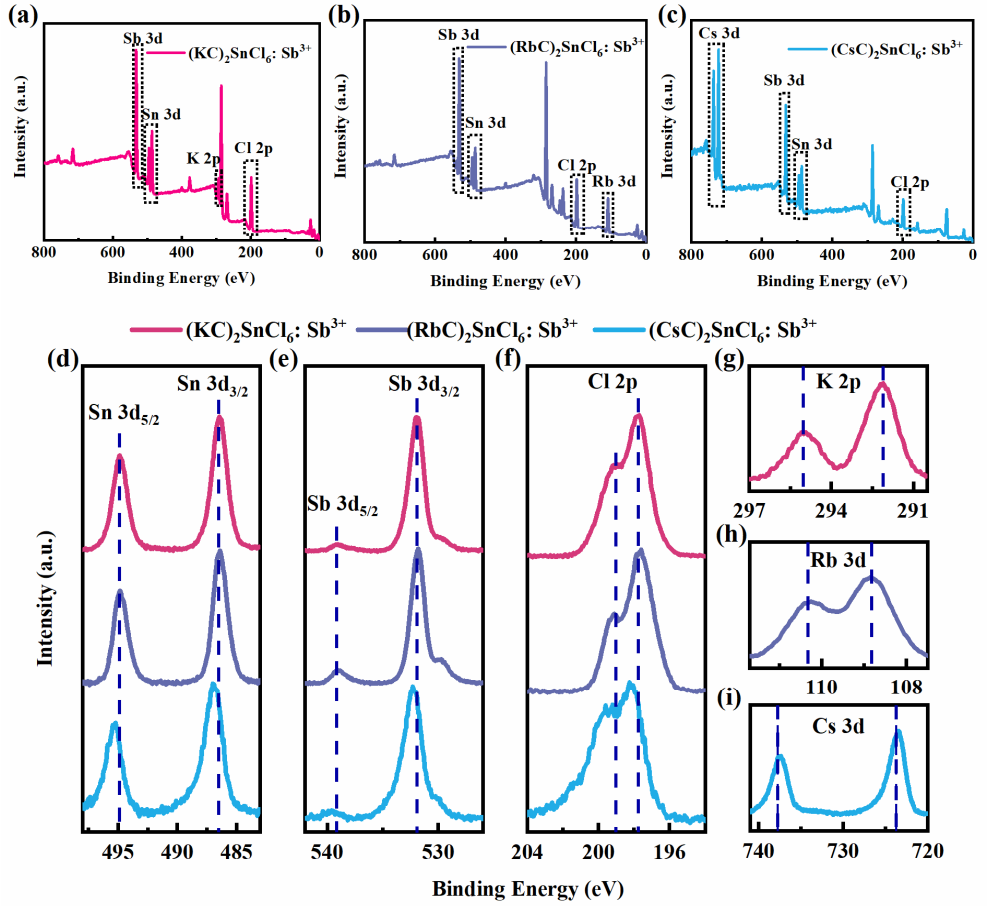

Fig. S2 High-resolution XPS spectra of (a-c)all, (d) Sn 3d, (e) Sb 3d, (f) Cl 2p of Sb^{3+}-doped $(AC)_2SnCl_6$, (g) K 2p of Sb^{3+}-doped $(KC)_2SnCl_6$, (h) Rb 3d of Sb^{3+}-doped $(RbC)_2SnCl_6$, and (i) Cs 3d of Sb^{3+}-doped $(CsC)_2SnCl_6$.

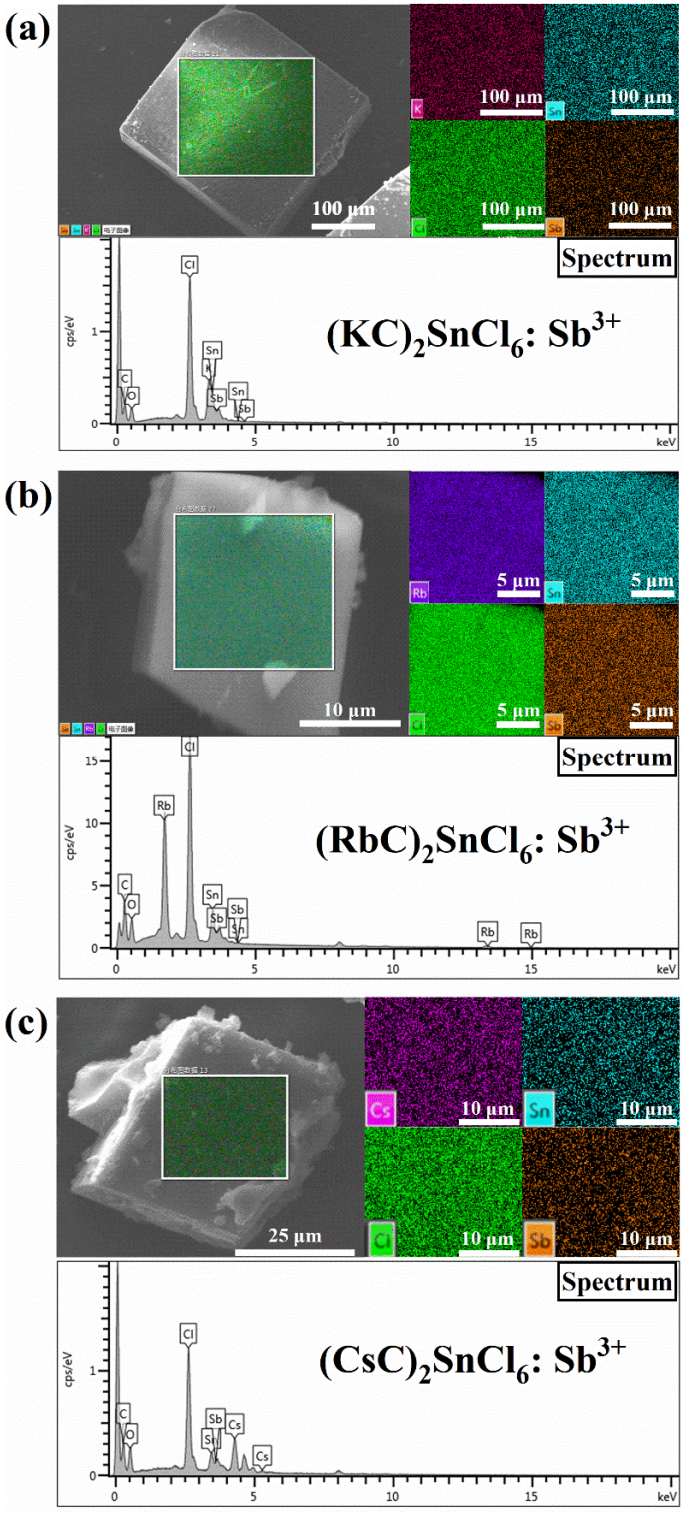

Fig. S3 SEM and EDS data of Sb^{3+} doped (a) $(KC)_2SnCl_6$, (b) $(RbC)_2SnCl_6$, and (c) $(CsC)_2SnCl_6$.

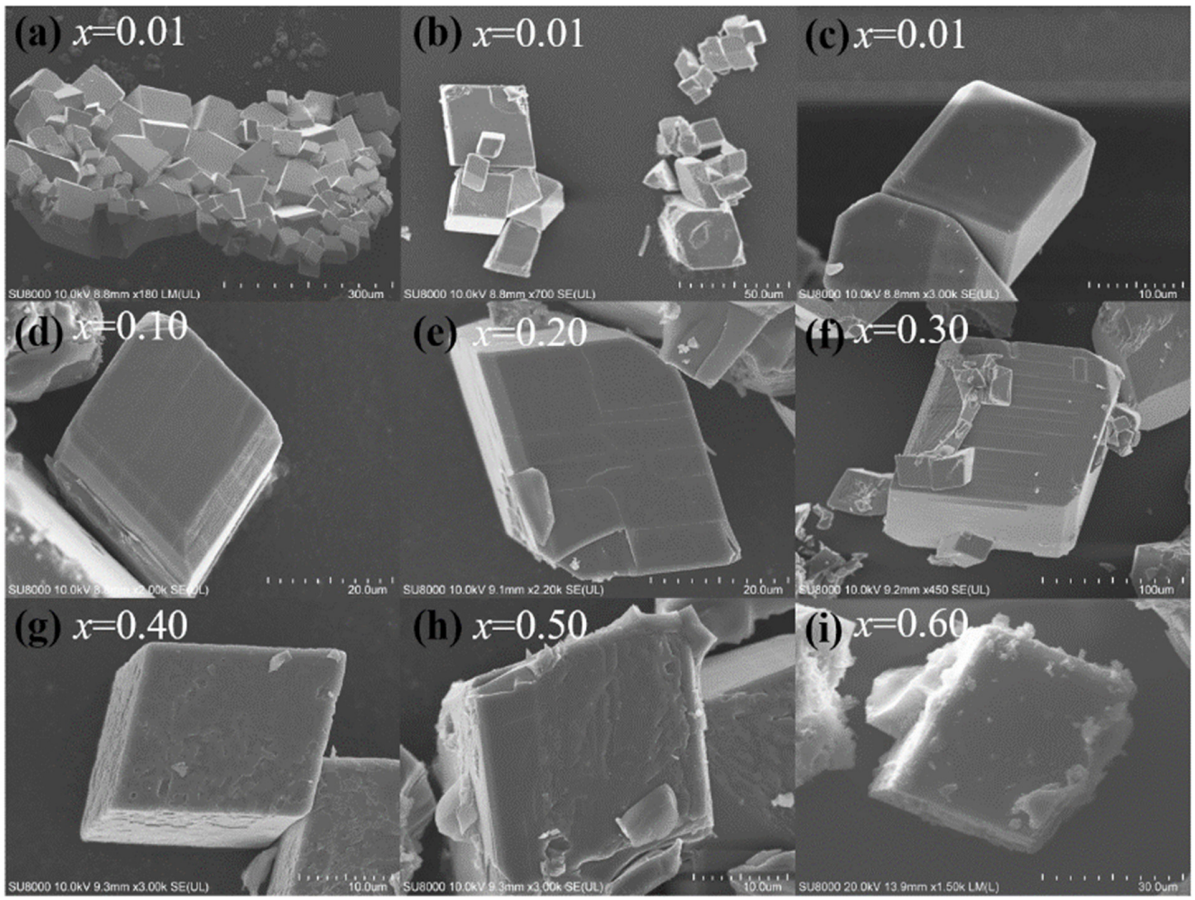

Fig. S4 SEM images of $(CsC)_2SnCl_6$: x% Sb^{3+} with various Sb^{3+} doping concentrations (x = 1-60).

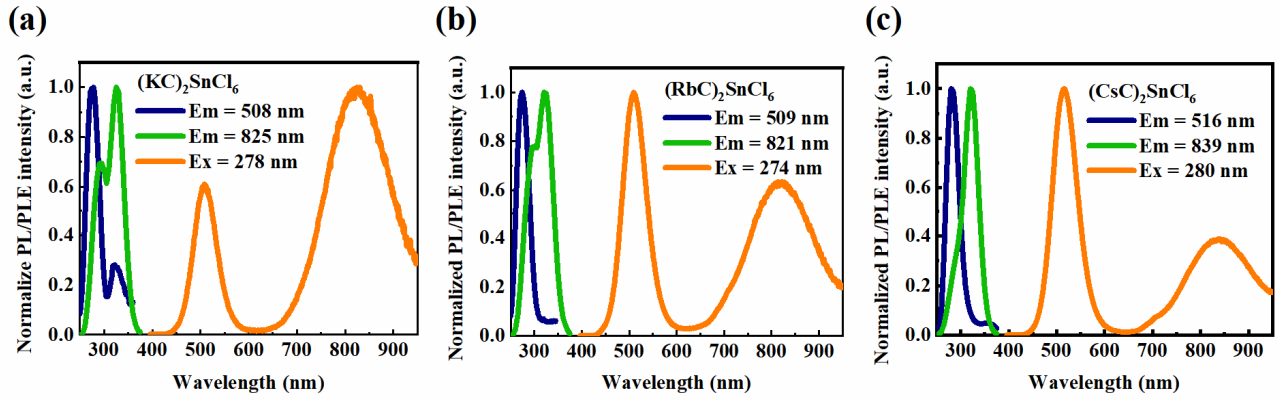

Fig. S5 PLE and PL spectra of (a) $(KC)_2SnCl_6$, (b) $(RbC)_2SnCl_6$, and (c) $(CsC)_2SnCl_6$.

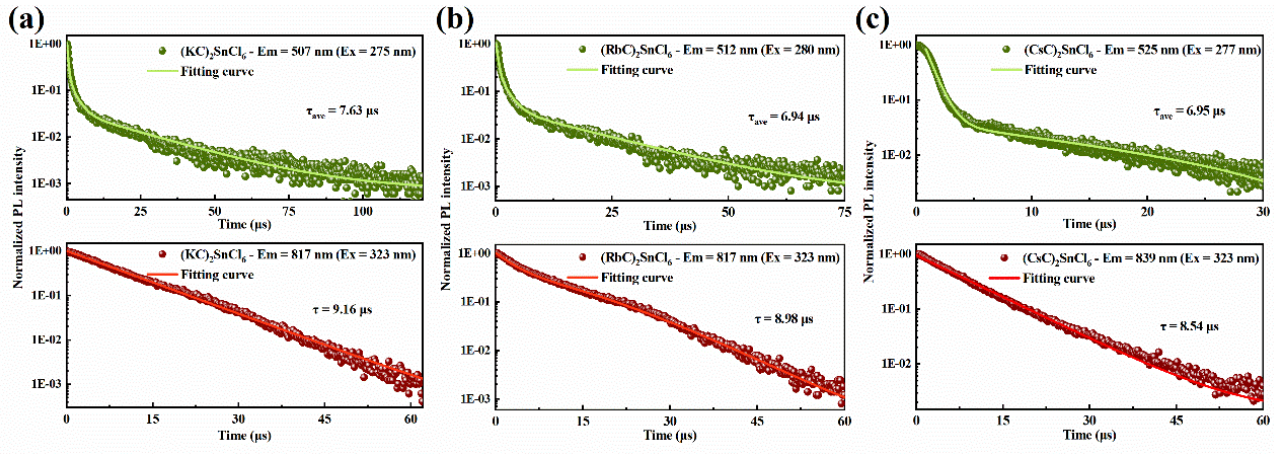

Fig. S6 Decay lifetimes of (a) $(KC)_2SnCl_6$, (b) $(RbC)_2SnCl_6$, and (c) $(CsC)_2SnCl_6$, monitored at high-energy emission band (top) and low-energy emission band, respectively (bottom).

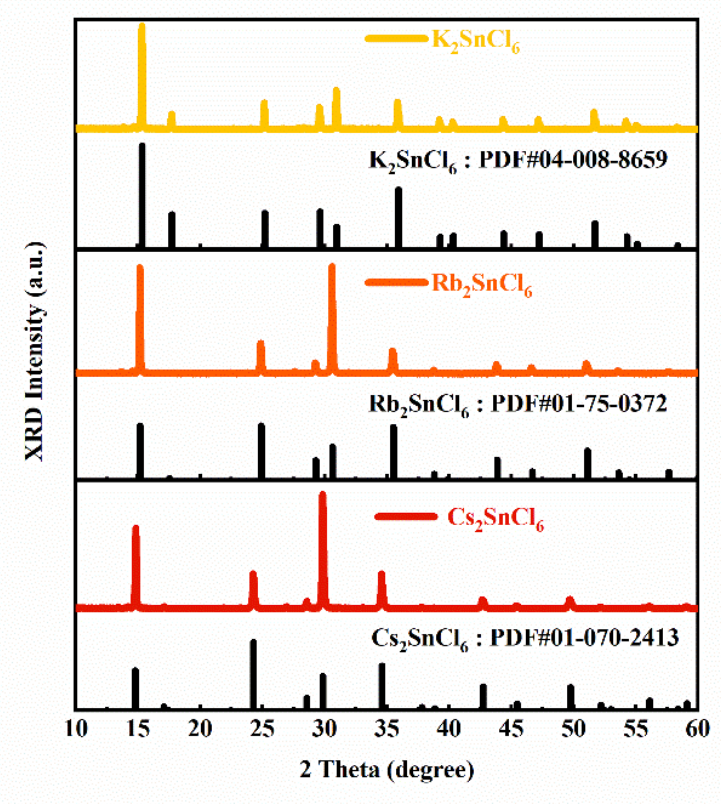

Fig. S7 Simulated and experimental PXRD results of A_2SnCl_6 (A = K, Rb, and Cs).

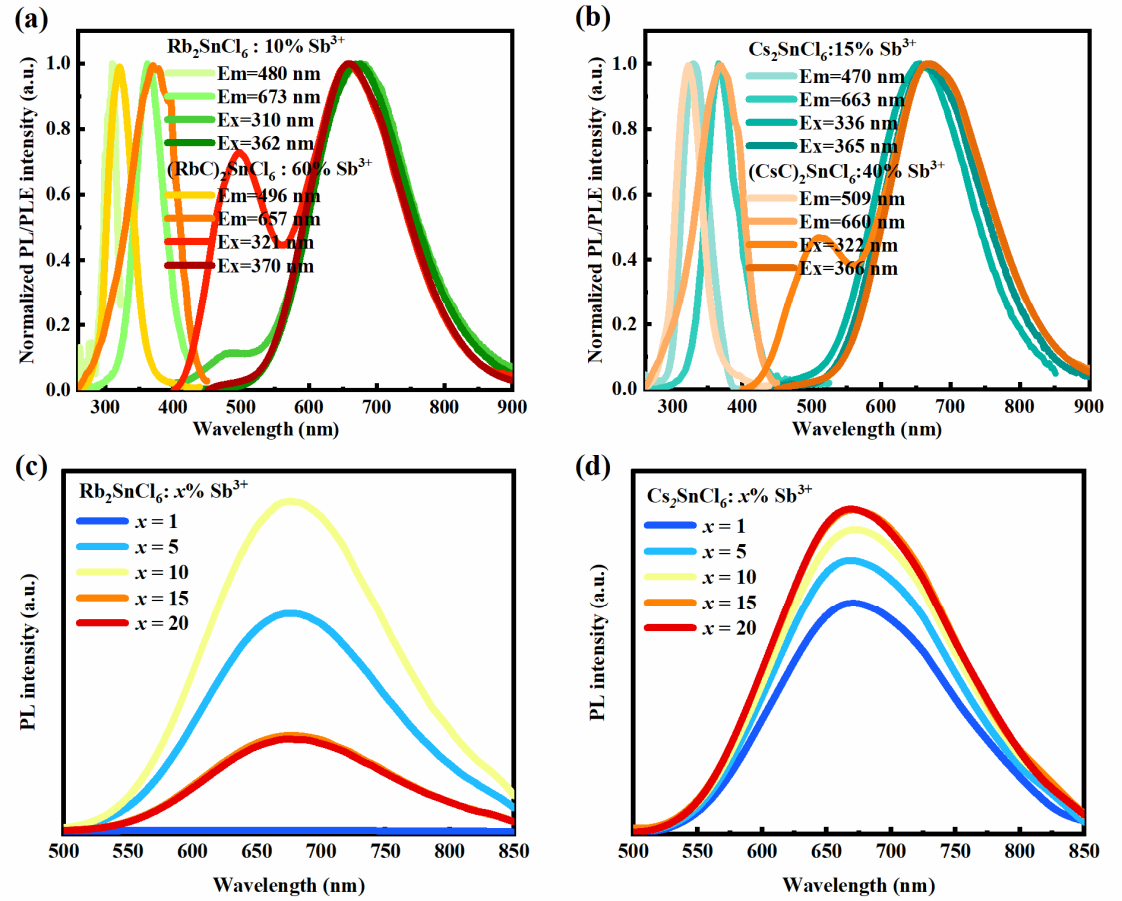

Fig. S8 Comparison of PL and PLE spectra between Sb^{3+}-doped (a) Rb_2SnCl_6 and $(RbC)_2SnCl_6$, and (b) Cs_2SnCl_6 and $(CsC)_2SnCl_6$. PL spectra of (c) Rb_2SnCl_6:x% Sb^{3+} and (d) Cs_2SnCl_6:x% Sb^{3+} under 365 nm excitation.

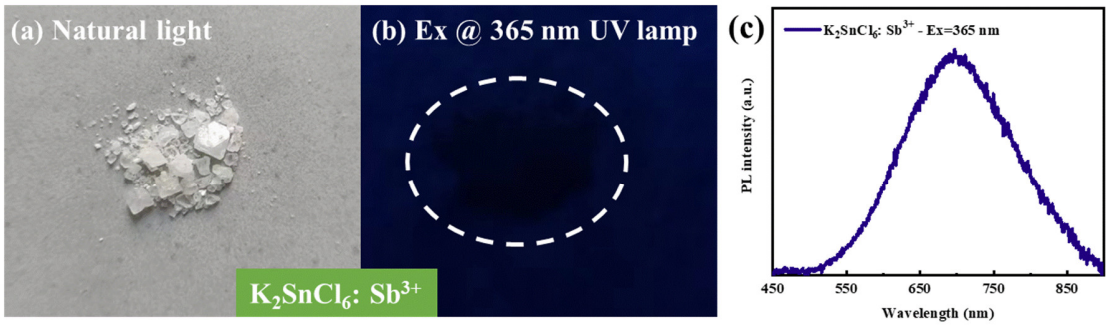

Fig. S9 Optical images of K_2SnCl_6: Sb^{3+} under (a) natural light and (b) 365 nm UV lamp. (c) PL spectrum of K_2SnCl_6: Sb^{3+} under 365 nm excitation.

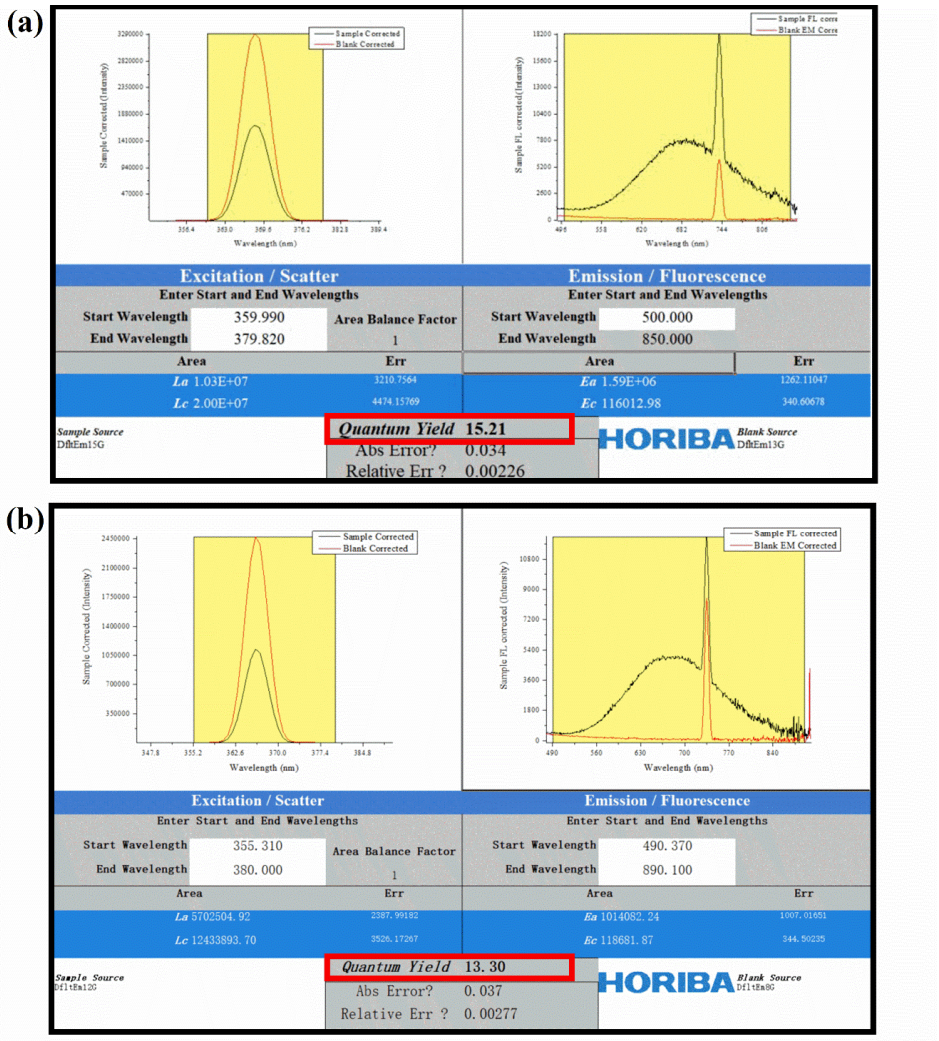

Fig. S10 PLQY of (a) Rb_2SnCl_6: 10% Sb^{3+} and (b) Cs_2SnCl_6: 15% Sb^{3+} under 365 nm excitation.

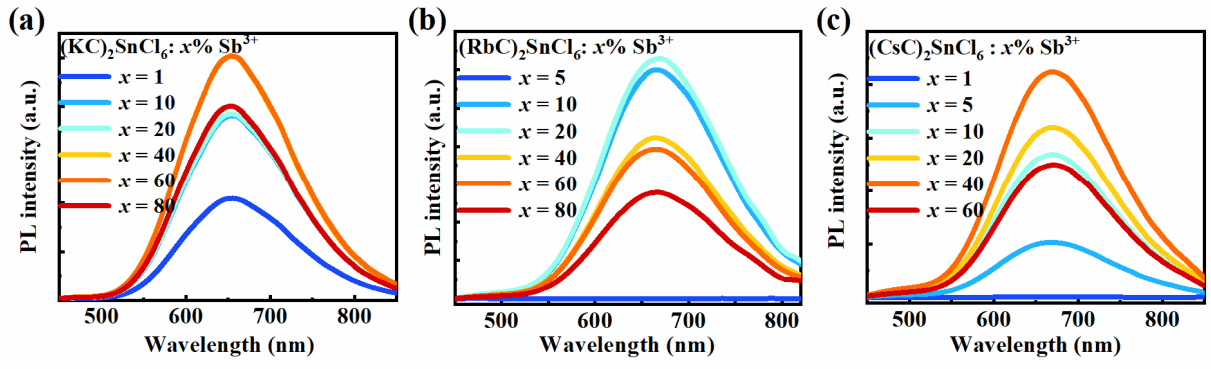

Fig. S11 PL spectra of varying doping concentrations of (a) $(KC)_2SnCl_6$:x% Sb^{3+}, (b) $(RbC)_2SnCl_6$:x% Sb^{3+} and (c) $(CsC)_2SnCl_6$:x% Sb^{3+}, under 370 nm excitation.

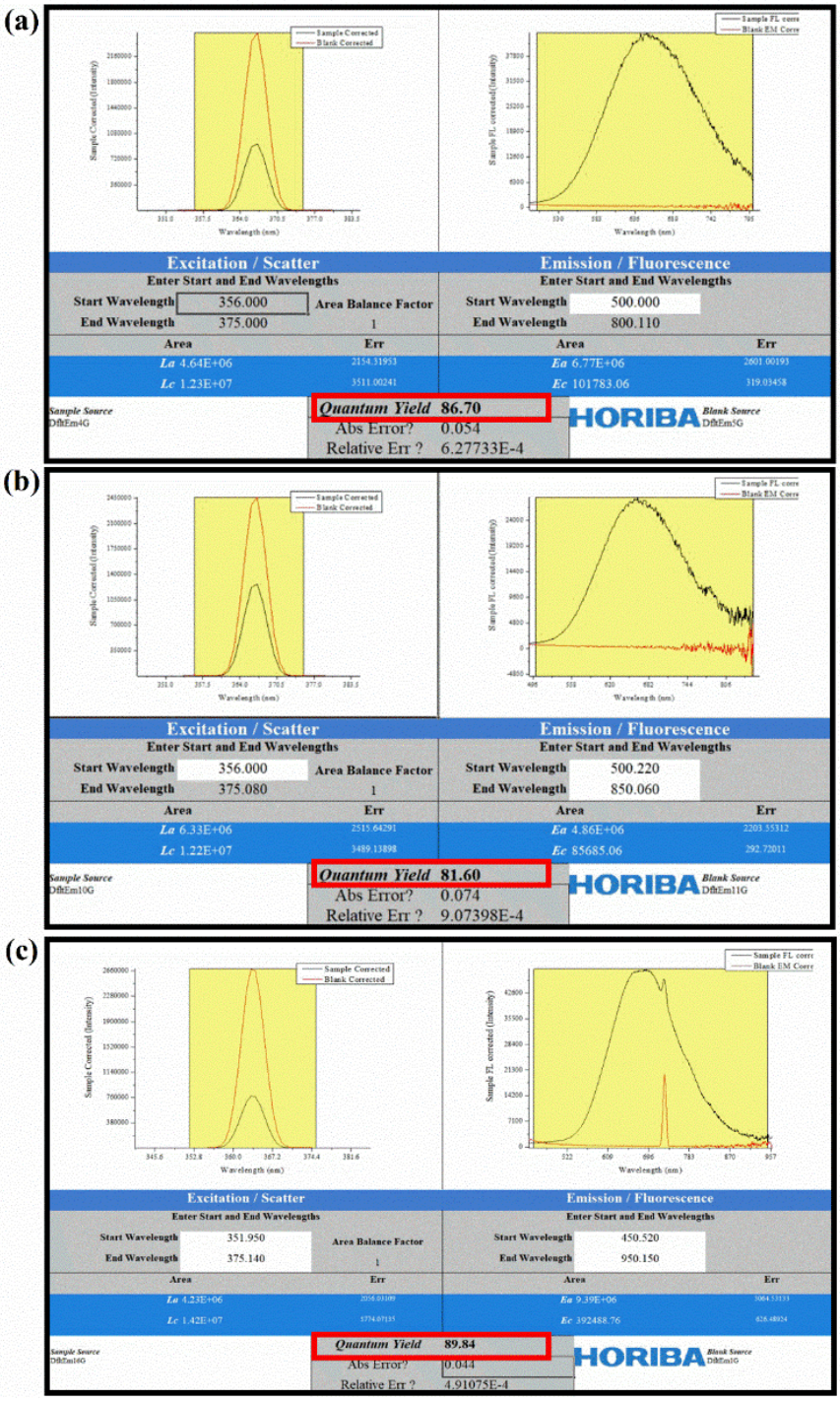

Fig. S12 PLQY of (a) $(KC)_2SnCl_6$: 60% Sb^{3+}, (b) $(RbC)_2SnCl_6$: 20% Sb^{3+}, and (c) $(CsC)_2SnCl_6$: 40% Sb^{3+} under 365 nm excitation.

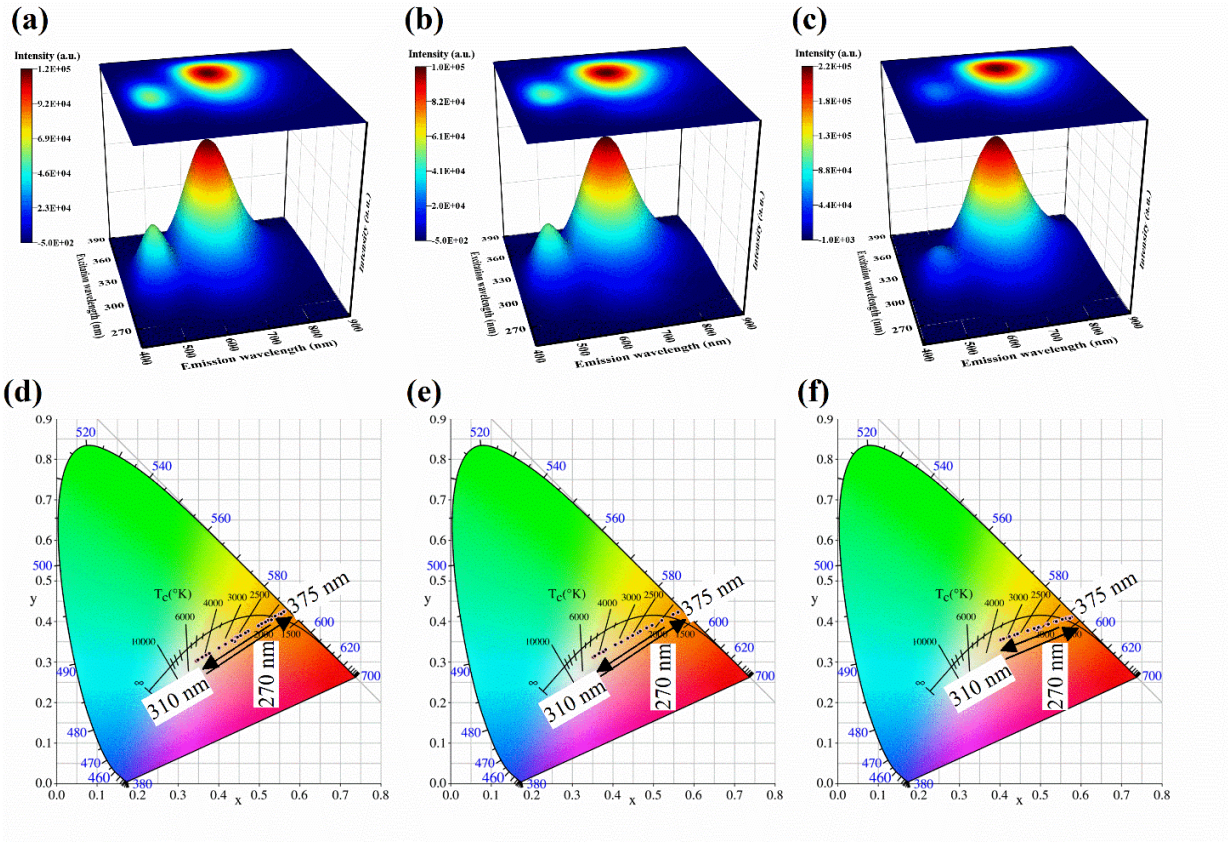

Fig. S13 PLE wavelength dependent PL spectra of $(AC)_2SnCl_6$: Sb^{3+}.

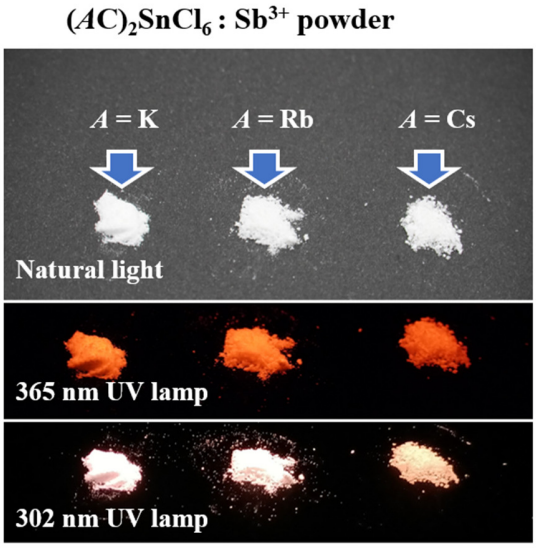

Fig. S14 Optical pictures of (a) $(CsC)_2SnCl_6$: Sb^{3+} crystals and (b) $(AC)_2SnCl_6$: Sb^{3+} (A = K, Rb, and Cs) powders under natural light, 365 nm, and 302 nm UV irradiation.

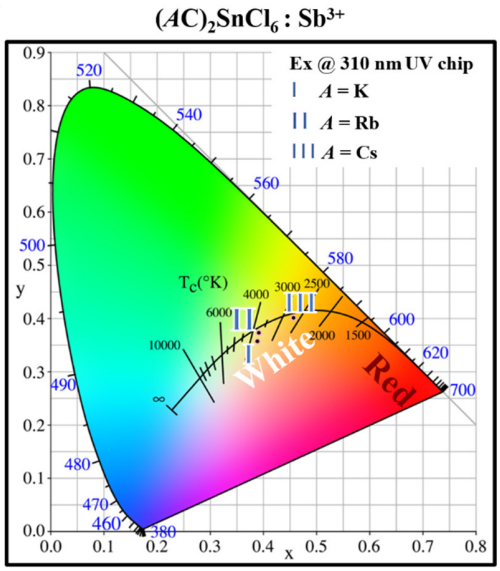

Fig. S15 CIE coordinates of the single-component WLED based on Sb^{3+}-doped $(AC)_2SnCl_6$ powders with a 310 nm UV chip.

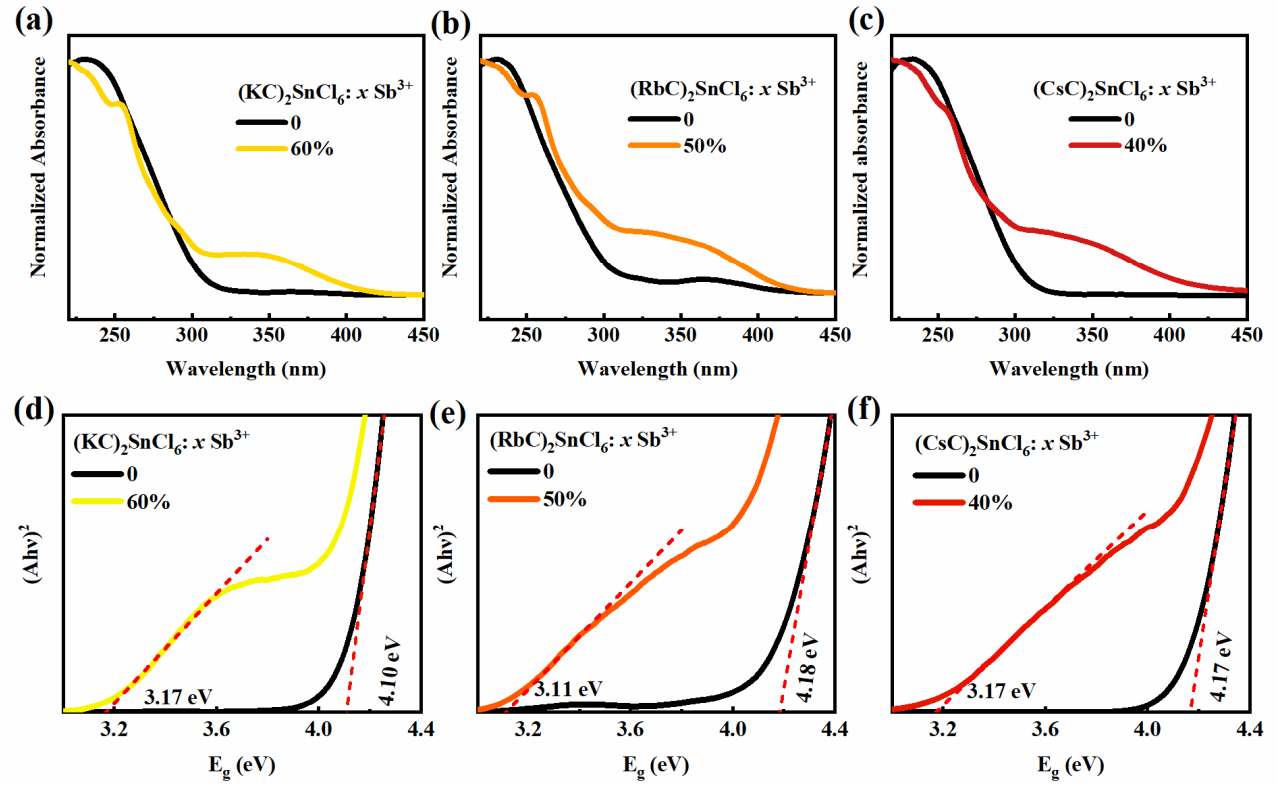

Fig. S16 (a-c) The (a-c) absorption spectra and (d,-f) the bandgap value determined by the Tauc plots of pristine and Sb^{3+} doped $(AC)_2SnCl_6$, A = K, Rb, and Cs, respectively.

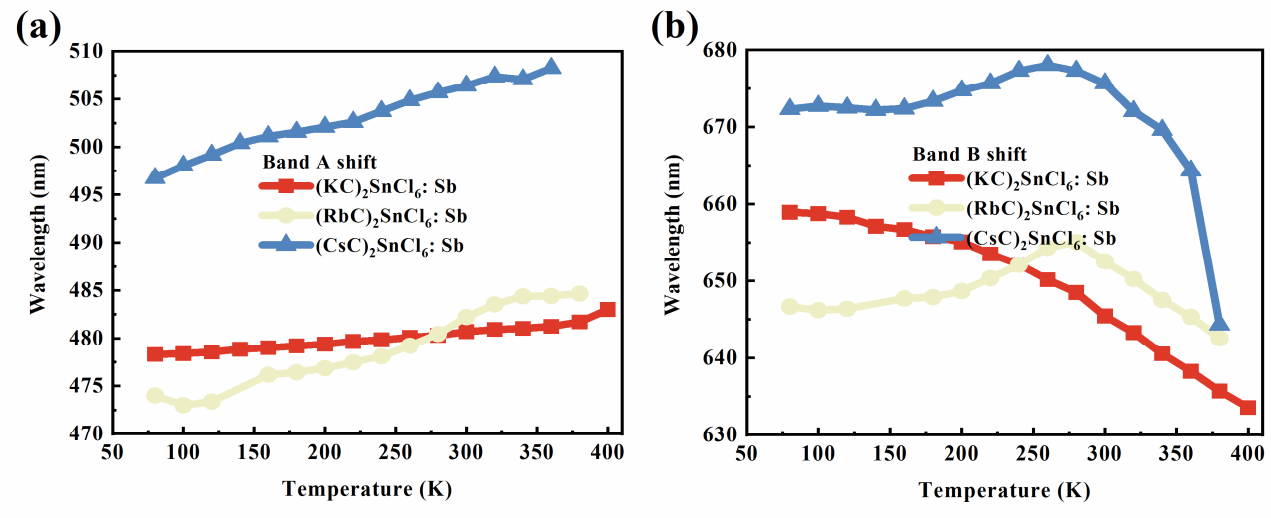

Fig. S17 The **Band A** and **Band B** position under various temperatures.

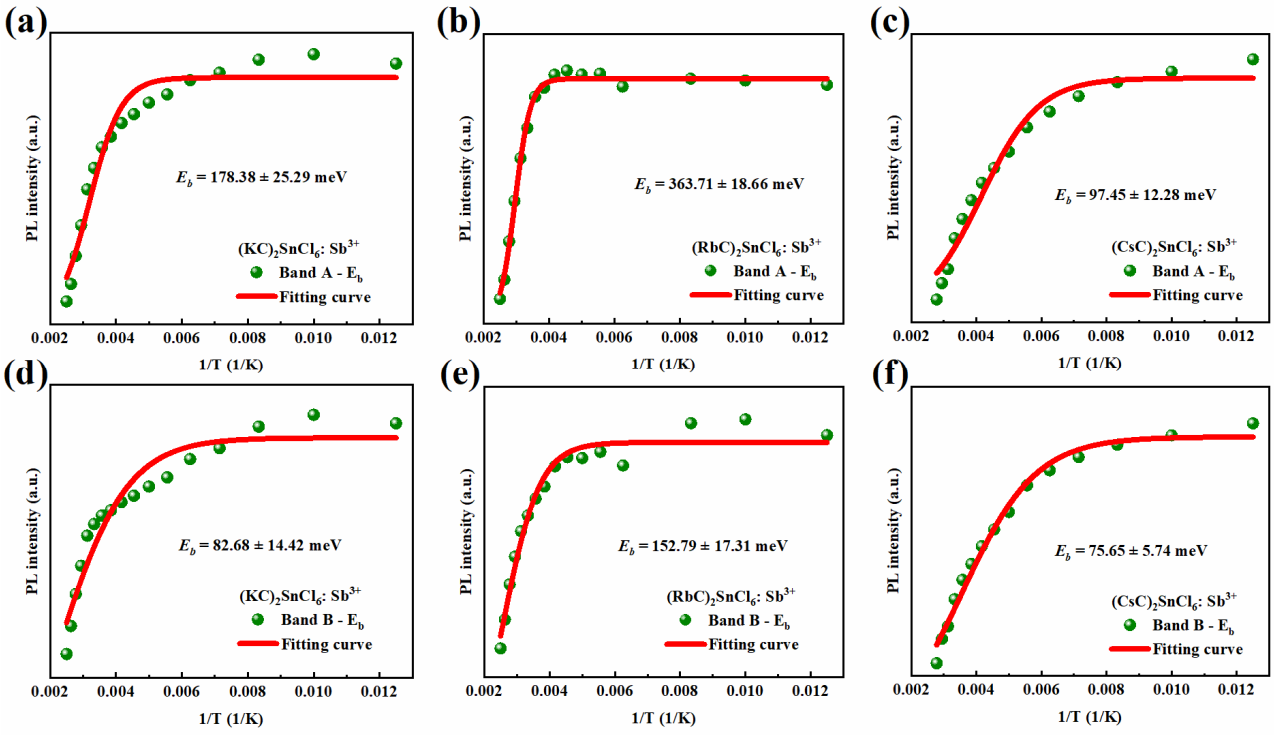

Fig. S18 Integrated PL intensity of (a-c) **Band A** and (d-f) **Band B** of **$(AC)_2SnCl_6$: Sb^{3+}** as a function of 1/T.

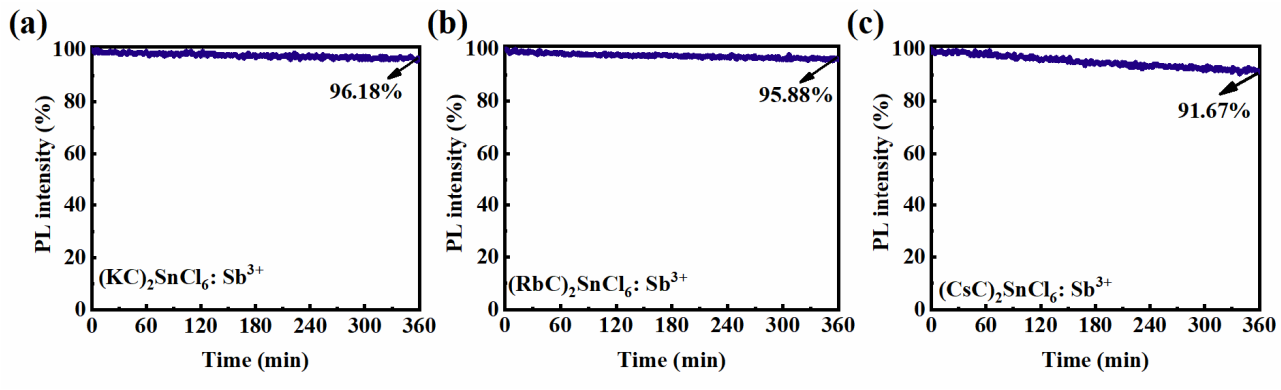

Fig. S19 PL stability of Sb^{3+}-doped (a) $(KC)_2SnCl_6$, (b) $(RbC)_2SnCl_6$, and (c) $(CsC)_2SnCl_6$ under 322 nm UV continuous illumination.

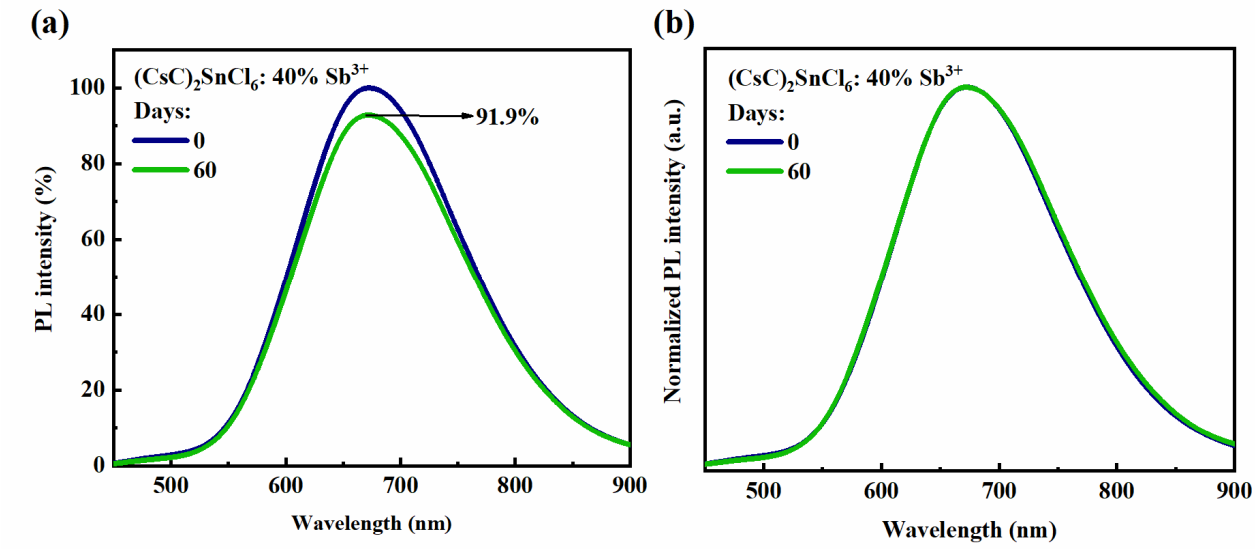

Fig. S20 (a) PL stability and (b) peak position of 40% Sb^{3+}-doped $(CsC)_2SnCl_6$ at pristine and after 60 days.

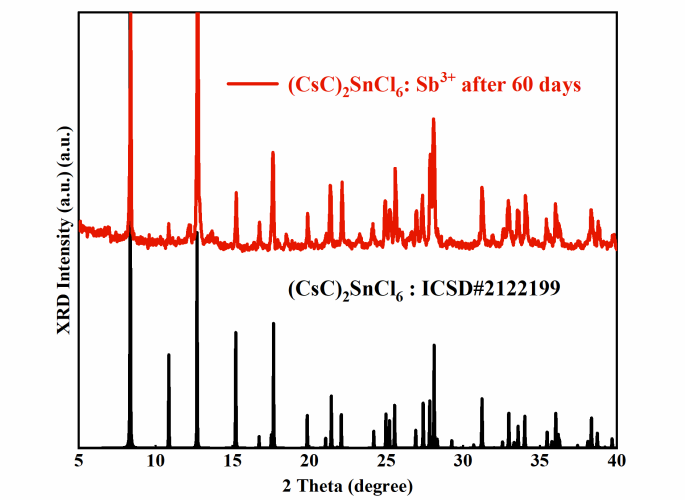

Fig. S21 PXRD patterns of the Sb^{3+}-doped $(CsC)_2SnCl_6$ powder stored at ambient 60 days (red), and the simulated of ICSD#2122199 (black).

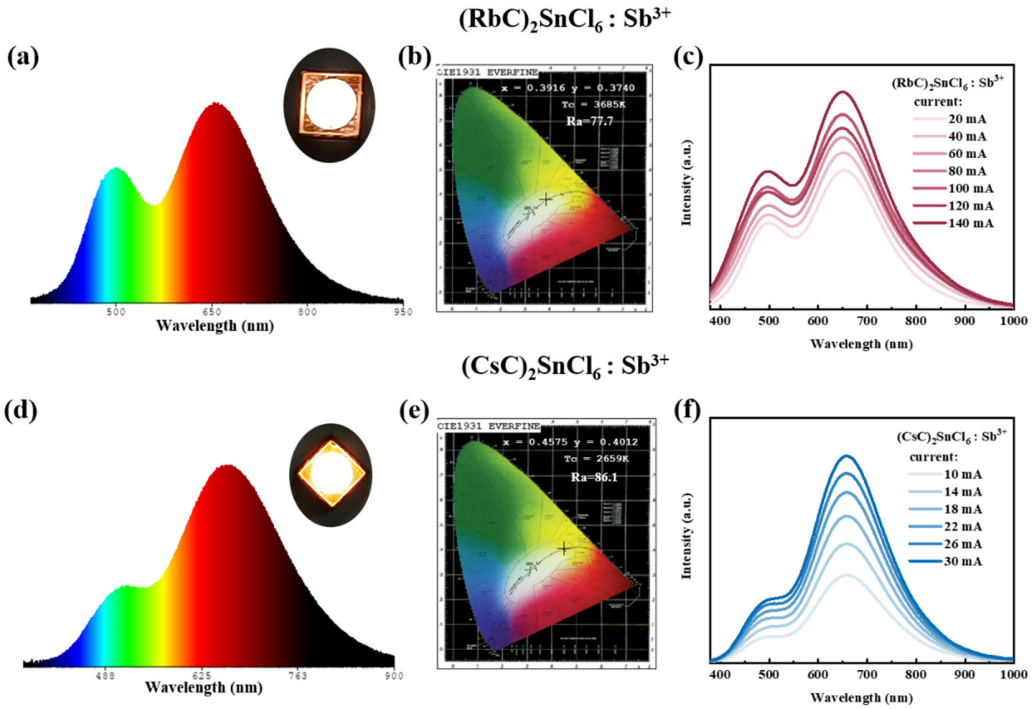

Fig. S22 Spectrum, WLED parameters, and drive current-dependent spectra of the single-component WLED based on Sb^{3+}-doped (a-c) $(RbC)_2SnCl_6$ and (d-f) $(CsC)_2SnCl_6$ powders, using a 310 nm UV chip. The inset in (a) and (d) exhibits the optical images of the WLED.

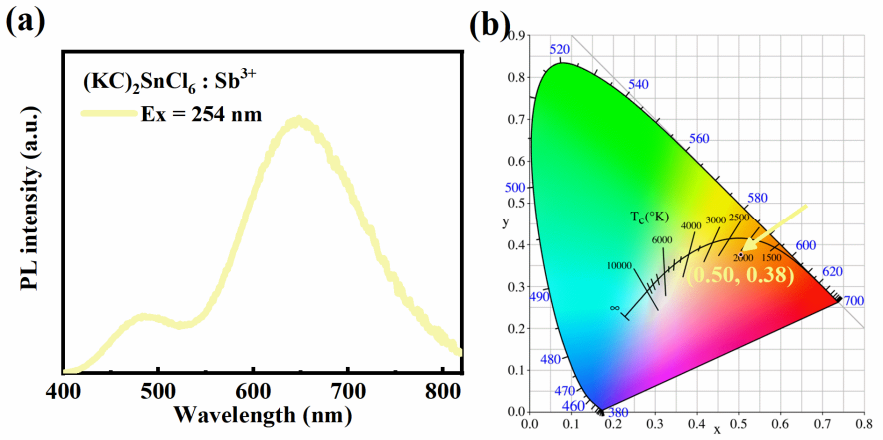

Fig. S23 PL spectrum and CIE coordinates of $(KC)_2SnCl_6$: Sb^{3+} under 254 nm UV excitation.

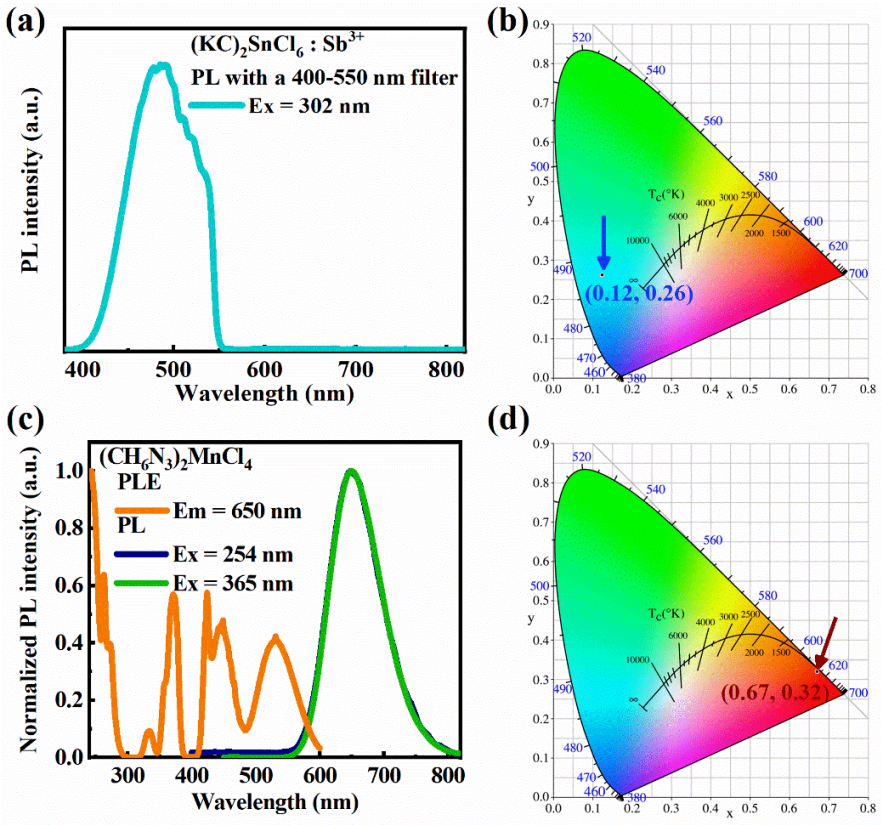

Fig. S24 PL spectrum (a) and CIE color coordinates (b) of $(KC)_2SnCl_6$: Sb^{3+} under 302 nm UV excitation with a 400-550 nm filter. PL and PLE spectra of $(CH_6N_3)_2MnCl_4$ (c) and the CIE color coordinates under 365 nm UV excitation.